

A minimization theorem for the Koide ratio and its Standard Model calibration

K. Hübner*

Independent researcher

(Dated: May 12, 2026)

arXiv:2605.09651v1 [hep-ph] 10 May 2026

Abstract

The charged-lepton Koide relation remains a striking empirical regularity in Standard-Model flavor data. We prove that for any positive mass set with Koide ratio Q_0 , the one-particle extension $Q(m_1, \dots, m_N, x)$ has a unique global minimum $Q_{\min} = Q_0/(1 + Q_0)$ at $m^* = [(\sum_i m_i)/(\sum_i \sqrt{m_i})]^2$. This exact kinematic result defines a unique extension benchmark. For the measured charged leptons it gives $m_*^\ell = 1.255\,34(16)$ GeV and $Q_{4,\min}^{\text{exp}} = 0.399\,997\,8(43)$; in the ideal Koide limit $Q_\ell^K = 2/3$, the corresponding minimum is exactly $2/5$. In the effective-participant language $N_{\text{eff}} \equiv 1/Q$, the optimal one-particle extension increases N_{eff} by one, while the equal- k multiplet extension increases it by k . The one-particle N_{eff} profile is exactly Lorentzian in a dimensionless share-mismatch coordinate u , which we interpret kinematically rather than dynamically. Using charged-lepton pole masses with the PDG 2024 own-scale $\overline{\text{MS}}$ charm mass gives $Q(e, \mu, \tau, c) = 0.400\,002\,5(64)$, i.e. 11.7 ppm above the measured-input benchmark and 6.2 ppm above $2/5$. This intentionally mixed-definition comparison is treated only as a phenomenological coincidence. To calibrate it within a stated benchmark class, we perform an exhaustive common-scale scan over non-neutrino Standard Model 2-body and 3-body seeds with one added mass. The charged-lepton-plus-charm continuation ranks 33/12,720 in the raw trial set, 24/2,640 after collapsing repeated scale realizations, and 6/756 within the fermion-only collapsed subset. We present the charm case as an empirically calibrated example of the theorem, not as a dynamical flavor model.

I. INTRODUCTION

In 1982 Koide observed that the three charged lepton masses satisfy, to remarkable accuracy, the dimensionless relation [1, 2]

$$Q \equiv \frac{m_e + m_\mu + m_\tau}{(\sqrt{m_e} + \sqrt{m_\mu} + \sqrt{m_\tau})^2} = \frac{2}{3}, \quad (1)$$

with a relative deviation of 9.3 ppm using PDG 2024 lepton masses [3]. Because Q is homogeneous of degree zero, it probes the relative placement of masses rather than their overall scale.

No symmetry of the Standard Model predicts Eq. (1). Foot reformulated the charged-lepton relation geometrically in terms of the angle between the \sqrt{m} vector and the demo-

* Corresponding author: k.a.huebner@web.de; ORCID: 0009-0001-6425-9527

cratic direction [4], while Sumino proposed a family-gauge mechanism that would protect the pole-mass relation against QED radiative corrections [5, 6], a proposal that is intrinsically tied to additional family-gauge dynamics not without phenomenological constraints. Various Koide-like extensions to running masses, quarks, and neutrinos have also been explored [7–14], with mixed phenomenological success. Because any a priori probability estimate for the charged-lepton coincidence depends strongly on the assumed prior over positive mass tuples, we do not assign a formal global significance to Eq. (1) here; instead, the only statistical calibration in this paper is the explicit look-elsewhere scan of Sec. VII.

This paper addresses a narrower question than a full flavor model: given a fixed positive mass multiplet, which extra mass minimizes the extended Koide ratio, and what does that imply for the observed charged leptons? We show that the answer is exact and model-independent: for any positive base set, $Q(m_1, \dots, m_N, x)$ has a unique global minimum at $x = m^*$, and the minimum value is $Q_0/(1+Q_0)$. Applied to the charged leptons, the theorem yields the measured-input benchmark $Q_{4,\min}^{\text{exp}}$ at the scale m_*^ℓ ; in the idealized world where the lepton Koide value is exactly $2/3$, the corresponding four-body minimum is exactly $2/5$. Accordingly, we reserve $Q_\ell^{\text{exp}} = Q(e, \mu, \tau) = 0.666\,661(12)$ for the measured charged-lepton ratio and $Q_\ell^K = 2/3$ for the idealized exact Koide value.

The theorem itself is the main new result of the paper. Earlier Koide literature has discussed empirical extensions to quarks, neutrinos, and running masses [7–14]; the point here is more specific. Rather than proposing another extension ansatz, we derive the unique extension point selected by minimizing the Koide ratio once a base tuple is held fixed.

Two reformulations of the same theorem turn out to be useful and are also new in this Koide-specific context. First, an equal-amplitude multiplet extension: when k additional masses are added with a common amplitude $r = \sqrt{x}$, the minimum is reached at the same $r^* = R_2/R_1$ as in the one-particle case and takes the closed form $Q_{\min}^{(k)} = Q_0/(1+kQ_0)$. Second, an *effective-participant* reading $N_{\text{eff}} \equiv 1/Q$ in which the one-particle theorem collapses to the additive identity $N_{\text{eff,max}} = N_{\text{eff,0}} + 1$ and its multiplet generalization to $N_{\text{eff,max}}^{(k)} = N_{\text{eff,0}} + k$; in particular the idealized lepton seed $N_{\text{eff,0}}^K = 3/2$ maps to the four-body benchmark $N_{\text{eff,max}}^K = 5/2$. This reading exposes that the kinematic content of the Koide ratio is a participation count rather than an energy scale. A third reformulation reparameterizes the one-particle extension curve in an exact Lorentzian coordinate $u(x) = (p - Q_{N+1,\min})/\sqrt{Q_{N+1,\min}(1 - Q_{N+1,\min})}$, where $p = r/(R_1 + r)$ is the normalized

amplitude share of the extender. This is an exact reparameterization of the kinematic curve, not a dynamical resonance, and gives the cleanest way to quote how close any candidate continuation sits to the theorem-selected peak. The same minimum is equivalently encoded geometrically in the Foot angle [4] between the \sqrt{m} vector and the democratic direction.

The phenomenological question is then whether any Standard Model mass lies close to that theorem-selected extension point. Using charged-lepton pole masses together with the short-distance charm mass $m_c(m_c)$, the PDG 2024 charm input lies 1.4% above m_*^ℓ and gives $Q(e, \mu, \tau, c) = 0.400\,002\,5$, which is 11.7 ppm above $Q_{4,\min}^{\text{exp}}$ and 6.2 ppm above the idealized value $2/5$. Because that comparison mixes lepton pole masses with a short-distance quark mass, and because other conventional charm-mass choices move the result away by 10^3 – 10^4 ppm, the observation must be treated as a mixed-definition phenomenological coincidence rather than a scheme-independent relation.

The main empirical task of this paper is therefore to calibrate that coincidence rather than to promote it to a new flavor law. We perform an exhaustive scan over all non-neutrino SM 2-body and 3-body seeds with one extra particle, evaluating any quark-containing trial in a common-scale $\overline{\text{MS}}$ setup. This shows whether the charged-lepton-plus-charm continuation is merely one entry in a broad pool of accidental near-minima, or whether it ranks high in this explicit benchmark ensemble. Charm is highlighted not because it is the numerically best Standard Model extension, but because it extends the already distinguished charged-lepton Koide triplet.

That benchmark ensemble is itself structured and partly a posteriori: it restricts attention to non-neutrino SM masses, to one-particle extensions of 2-body and 3-body seeds, and to the conventional common scales $\mu \in \{2\text{ GeV}, m_c, m_b, m_Z, m_t\}$ for quark-containing trials. The resulting scan fractions are therefore best read as rank statistics within this chosen comparison class, not as prior probabilities for flavor models or spectra.

The paper is organized as follows. Section II proves the exact one-particle minimization theorem and its equal-amplitude multiplet extension. Section III develops the concentration-measure, effective-participant ($N_{\text{eff}} = 1/Q$), and exact Lorentzian-coordinate reformulations of the extension problem, including the idealized $Q_\ell^K = 2/3 \rightarrow Q_{4,\min}^K = 2/5$ (equivalently $N_{\text{eff},0}^K = 3/2 \rightarrow N_{\text{eff,max}}^K = 5/2$) corollary. Section IV then applies that setup to the measured charged leptons and quantifies the charm comparison. Section V examines the scheme dependence of that mixed-definition input choice. Section VI recasts the charm discussion in

Foot’s angular language and quantifies the theorem-selected continuation angle. Section VII gives the look-elsewhere calibration from the exhaustive 2-body and 3-body scan, where the charged-lepton-plus-charm continuation ranks 24/2,640 in the full collapsed leaderboard and 6/756 within the fermion-only sub-ensemble. Section VIII summarizes the outcome and its limitations.

We use natural units throughout. Quark masses are $\overline{\text{MS}}$ values from PDG 2024 [3] unless otherwise stated. Lepton masses are on-shell (pole) masses, which is also the empirical input convention in which the charged-lepton Koide relation is usually quoted. When charm is added, we use the short-distance quantity $m_c(m_c)$ as the default reference because a charm pole mass is not a comparably clean observable. The resulting lepton-pole plus $\overline{\text{MS}}$ -charm comparison is therefore a practical mixed-definition convention rather than a model-derived common scheme. Unless stated otherwise, quoted ppm deviations from a reference value X_{ref} mean the signed relative difference $10^6(X - X_{\text{ref}})/X_{\text{ref}}$; when only closeness matters, we quote the magnitude. Phrases such as “ X ppm above X_{ref} ” are used as a verbal shorthand for a positive value of the same signed relative difference, not as a separate inequality statement. Quoted uncertainties are propagated at leading order from the stated input mass errors using diagonal Gaussian error propagation. We neglect input correlations throughout and use the resulting numbers only as local sensitivity estimates rather than as full statistical intervals. Neutrinos are excluded from the scan below because only mass splittings, not a unique absolute-mass spectrum, are experimentally established; any neutrino leaderboard would therefore build in additional assumptions that are not needed for the present charged-lepton benchmark.

II. THE Q -MINIMUM THEOREM

Theorem 1. *Let $m_i > 0$ be particle masses and let $r_i = \sqrt{m_i}$ for $i = 1, \dots, N$. Define*

$$R_1 \equiv \sum_{i=1}^N r_i, \quad R_2 \equiv \sum_{i=1}^N r_i^2 = \sum_{i=1}^N m_i, \quad Q_0 \equiv Q_N(\{m_i\}) = \frac{R_2}{R_1^2}.$$

Here Q_0 is simply the Koide ratio of the unextended base tuple. For an added mass x written as $r = \sqrt{x} > 0$, consider the extended ratio

$$Q_{N+1}(r) = \frac{R_2 + r^2}{(R_1 + r)^2}. \quad (2)$$

Then:

(i) Q_{N+1} has a unique global minimum at

$$r^* = \frac{R_2}{R_1} = Q_0 R_1, \quad m^* = (r^*)^2 = \left(\frac{\sum_i m_i}{\sum_i \sqrt{m_i}} \right)^2, \quad (3)$$

(ii) The minimum value is

$$Q_{\min} = \frac{Q_0}{1 + Q_0}. \quad (4)$$

Proof. Differentiating Eq. (2) with respect to r gives

$$\frac{dQ_{N+1}}{dr} = \frac{2(R_1 r - R_2)}{(R_1 + r)^3} = \frac{2R_1(r - r^*)}{(R_1 + r)^3}. \quad (5)$$

In particular, $dQ_{N+1}/dr = 0$ at $r = r^*$. Since $R_1 > 0$ and $R_1 + r > 0$, the derivative is negative for $0 < r < r^*$ and positive for $r > r^*$, so r^* is the unique global minimum. Substituting $R_2 = Q_0 R_1^2$ and $r^* = Q_0 R_1$ gives

$$\begin{aligned} Q_{\min} &= \frac{R_2 + (r^*)^2}{(R_1 + r^*)^2} = \frac{Q_0 R_1^2 + Q_0^2 R_1^2}{R_1^2 (1 + Q_0)^2} \\ &= \frac{Q_0 + Q_0^2}{(1 + Q_0)^2} = \frac{Q_0}{1 + Q_0}. \quad \square \end{aligned} \quad (6)$$

□

For any positive $(N + 1)$ -tuple, the Cauchy–Schwarz inequality gives $R_1^2 \leq (N + 1)R_2$ and hence $Q_{N+1} \geq 1/(N + 1)$. For any positive $(N + 1)$ -tuple with $N + 1 \geq 2$, one has $R_1^2 = R_2 + 2 \sum_{i < j} r_i r_j > R_2$, so $Q_{N+1} < 1$; for the trivial one-mass case one instead has $Q_1 = 1$. The theorem above does not require the m_i to be distinct; degenerate base masses ($m_i = m_j$ for some $i \neq j$) are allowed, in which case the r_i -weighted barycenter r^* remains a well-defined positive number. With the first N masses fixed, however, an extension generally cannot reach the absolute lower bound $1/(N + 1)$; its sharp lower bound is instead the theorem value $Q_{\min} = Q_0/(1 + Q_0)$. Since every positive N -tuple satisfies $Q_0 \geq 1/N$, one has

$$Q_{\min} = \frac{Q_0}{1 + Q_0} \geq \frac{1}{N + 1}. \quad (7)$$

Equality holds only in the trivial equal-mass limit.

Three brief readings of $r^* = R_2/R_1$ are useful. First, $R_1 r^* - R_2 = \sum_i r_i (r^* - r_i) = 0$ shows that r^* is the r_i -weighted barycenter of the base r_i on the positive line. Equivalently, if one

regards the r_i as a weighted sample with weights proportional to r_i , then r^* is their weighted mean and the minimum condition is the vanishing of the corresponding weighted first central moment. Because r^* is a positive weighted mean of the base mass amplitudes $r_i = \sqrt{m_i}$, it necessarily lies between the smallest and largest r_i ; equivalently, the minimizing mass $m^* = (r^*)^2$ lies between the smallest and largest base masses. Second, in Foot's democratic-vector language [4], the allowed extension line $W(r) = (r_1, \dots, r_N, r)$ reaches its least-deviating alignment with the democratic direction precisely at $r = r^*$. We return to this geometric interpretation in Sec. VI. Third, the theorem also admits an exact concentration-measure reading. Because $Q_0 = \sum_i p_i^2 = \text{tr}(\rho^2)$ for the normalized amplitude weights $p_i = r_i/R_1$, it can be read as a purity or inverse participation measure on the probability simplex. We return to that interpretation, and to the associated effective-participant coordinate $N_{\text{eff}} \equiv 1/Q$, in Sec. III.

The same minimizer also controls the equal-multiplet extension problem: if one adds k new masses and minimizes over their corresponding r -variables jointly, the global minimum occurs when they are all equal to the same r^* , giving $Q_{\text{min}}^{(k)} = Q_0/(1 + kQ_0)$. To see this, let the new mass amplitudes be $s_1, \dots, s_k > 0$ and define $S \equiv \sum_{a=1}^k s_a$. For fixed S , one has $\sum_a s_a^2 \geq S^2/k$, with equality only when all $s_a = S/k$. The multi-particle problem therefore reduces to minimizing

$$\tilde{Q}_{N+k}(S) = \frac{R_2 + S^2/k}{(R_1 + S)^2} \quad (8)$$

over $S > 0$. Differentiating gives

$$\frac{d\tilde{Q}_{N+k}}{dS} = \frac{2(R_1 S - kR_2)}{k(R_1 + S)^3}, \quad (9)$$

so the unique minimum occurs at $S^* = kR_2/R_1$, i.e. at $s_1 = \dots = s_k = R_2/R_1 = r^*$. Substituting back yields

$$Q_{\text{min}}^{(k)} = \frac{R_2 + k(r^*)^2}{(R_1 + kr^*)^2} = \frac{Q_0}{1 + kQ_0}. \quad (10)$$

Thus repeated exact minimization keeps returning to the same optimal scale and approaches the large- N lower bound $Q_N \sim 1/N$ from above.

Equation (3) is the only ingredient needed for the phenomenology below: once a base tuple is fixed, the theorem selects a unique extension scale m^* and an equally unique benchmark value Q_{min} . The question is then empirical rather than formal: whether any known SM mass lies unusually close to that theorem-selected point. If the charged-lepton Koide relation

reflects real flavor structure rather than accident, then this minimizer can be read as the unique least-disruptive one-particle continuation of that structure. We do not develop such a model here; we use the theorem only as a benchmark.

III. EFFECTIVE-PARTICIPANT AND LORENTZIAN COORDINATES

Beyond the minimizing mass itself, the theorem has useful exact corollaries for concentration measures and for the idealized charged-lepton Koide limit. In this section $Q_\ell^K = 2/3$ denotes the idealized exact charged-lepton Koide value; the corresponding measured-input benchmarks are introduced later in Sec. IV.

The theorem has a compact reading in terms of concentration measures. Define normalized amplitude weights $p_i = r_i/R_1 \geq 0$ with $\sum_i p_i = 1$; the weights live on the probability simplex Δ^{N-1} . Packaging them into the diagonal probability matrix $\rho \equiv \text{diag}(p_1, \dots, p_N)$, one has

$$Q_0 = \text{tr}(\rho^2) = \sum_i p_i^2, \quad (11)$$

equivalently the Herfindahl–Hirschman concentration index [15] or the squared ℓ^2 norm of $\{p_i\}$. In the present classical setting this same quantity is simply the collision probability, i.e. the probability that two independent draws from $\{p_i\}$ return the same family index. It is smallest at the equal-mass point $p_i = 1/N$, where $\rho = 1/N$ and $Q_0 = 1/N$, and it tends to 1 as a single mass dominates. The exact charged-lepton Koide value $Q_\ell^K = 2/3$ is therefore the statement that the charged-lepton \sqrt{m} profile has purity $2/3$, well above the three-mass equal-mass floor of $1/3$.

The extended ratio is

$$Q_{N+1}(r) = \frac{R_2 + r^2}{(R_1 + r)^2}, \quad (12)$$

minimized at $r^* = Q_0 R_1 = R_2/R_1$. So the minimizing amplitude is the base purity times the total base amplitude R_1 . The resulting amplitude profile is

$$p_i^* = (1 - Q_{\min})p_i, \quad p_{N+1}^* = Q_{\min} \quad (13)$$

so the old distribution is uniformly rescaled while the new particle absorbs exactly the final purity. The rescaling factor follows from $R_1 + r^* = R_1(1 + Q_0) = R_1/(1 - Q_{\min})$.

Because Q is itself a purity, its inverse has a direct counting interpretation, and the theorem takes its simplest form in that language. Define the *effective participant number*

$$N_{\text{eff}} \equiv \frac{1}{Q}. \quad (14)$$

It equals N for the uniform distribution (all N amplitudes contribute equally) and approaches 1 as one amplitude dominates. Equivalently, N_{eff} is the size of the hypothetical equal-weight distribution that has the same purity as $\{p_i\}$. For the base tuple $N_{\text{eff},0} = 1/Q_0$ and for the peak value reached at the minimizing extension $N_{\text{eff,max}} = 1/Q_{\text{min}}$, the relation $Q_{\text{min}} = Q_0/(1 + Q_0)$ is simply

$$N_{\text{eff,max}} = N_{\text{eff},0} + 1. \quad (15)$$

So the optimal one-particle extension increases the effective participant number by exactly one. For the exact charged-lepton Koide value $Q_\ell^K = 2/3$, one has $N_{\text{eff},0}^K = 3/2$; after the optimal extension,

$$Q_{4,\text{min}}^K = \frac{Q_\ell^K}{1 + Q_\ell^K} = \frac{2}{5} \quad (16)$$

and therefore $N_{\text{eff,max}}^K = 5/2$.

The same language extends immediately to the equal- k multiplet theorem. If k new amplitudes are added and minimized jointly, the result $Q_{\text{min}}^{(k)} = Q_0/(1 + kQ_0)$ reads

$$N_{\text{eff,max}}^{(k)} = N_{\text{eff},0} + k. \quad (17)$$

Each of the k optimal particles therefore contributes exactly one unit to the effective participant number.

The same effective-participant language also admits a useful exact shape reparameterization for the one-particle extension curve. For fixed base amplitudes and an added amplitude $r = \sqrt{x}$,

$$N_{\text{eff}}(r) = \frac{(R_1 + r)^2}{R_2 + r^2}. \quad (18)$$

Defining the dimensionless extension strength

$$s \equiv \frac{r}{R_1} \quad (19)$$

and the new particle's normalized amplitude share

$$p_X \equiv \frac{r}{R_1 + r} = \frac{s}{1 + s}, \quad (20)$$

one may introduce the standardized share-mismatch coordinate

$$u \equiv \frac{p_X - Q_{\min}}{\sqrt{Q_{\min}(1 - Q_{\min})}}. \quad (21)$$

Here s , p_X , and u are all dimensionless. The variable s measures the new amplitude against the total coherent base amplitude, p_X is the new state's share of the total normalized \sqrt{m} weight, and u measures the deviation of that share from the theorem-selected value in units of the natural Bernoulli width $\sqrt{Q_{\min}(1 - Q_{\min})}$. A direct calculation gives the exact identity

$$Q(p_X) = p_X^2 + Q_0(1 - p_X)^2 = Q_{\min} + \frac{(p_X - Q_{\min})^2}{1 - Q_{\min}}, \quad (22)$$

i.e. Q is exactly quadratic in the share p_X , with minimum $Q_{\min} = Q_0/(1+Q_0)$ at $p_X = Q_{\min}$. Substituting the u coordinate of Eq. (21) into Eq. (22) gives $Q(u) = Q_{\min}(1 + u^2)$, and hence

$$N_{\text{eff}}(u) = \frac{N_{\text{eff,max}}}{1 + u^2} \quad \text{with} \quad N_{\text{eff,max}} = \frac{1}{Q_{\min}}. \quad (23)$$

The Lorentzian form is therefore not an independent observation but a direct algebraic consequence of the exact quadratic dependence (22) together with the inversion $N_{\text{eff}} = 1/Q$. The normalized peak is an exact Lorentzian, $N_{\text{eff}}/N_{\text{eff,max}} = 1/(1 + u^2)$. Its maximum occurs at $u = 0$, where $N_{\text{eff}}(0) = N_{\text{eff,max}}$. Its half-maximum occurs at $|u| = 1$, and the inflection points are the universal values $u = \pm 1/\sqrt{3}$, independent of the base tuple. This universal profile will be evaluated for the measured charged-lepton base in Sec. IV.

This Lorentzian form should be read kinematically, not dynamically. It does *not* imply an unstable state, a decay width, or a literal Breit–Wigner resonance in flavor space. Its value is instead interpretive: after the nonlinear coordinate change of Eq. (21), the entire one-particle extension problem is reduced to a universal even function of the deviation from the theorem-selected amplitude share. In that sense u is a natural dimensionless mismatch coordinate for any future dynamical model that attempts to realize the least-disruptive continuation of a Koide-special base tuple.

IV. LEPTON EXTENSION AND THE CHARM SCALE

We now turn to the measured charged-lepton spectrum. In this section, Q_ℓ^{exp} denotes the charged-lepton Koide ratio computed from the measured PDG 2024 pole masses, while $Q_\ell^K = 2/3$ remains the idealized exact Koide value used for comparison, with corresponding

theorem-selected four-body benchmark $Q_{4,\min}^K = Q_\ell^K/(1 + Q_\ell^K) = 2/5$. Using the PDG 2024 charged-lepton pole masses and hence $Q_\ell^{\text{exp}} = 0.666\,661(12)$ [3],

$$Q_{4,\min}^{\text{exp}} = \frac{Q_\ell^{\text{exp}}}{1 + Q_\ell^{\text{exp}}} = 0.399\,997\,8(43). \quad (24)$$

Equivalently, the measured charged-lepton seed has $N_{\text{eff},0}^{\text{exp}} = 1/Q_\ell^{\text{exp}} = 1.500014(27)$ and the theorem-selected four-body peak value is $N_{\text{eff},\max}^{\text{exp}} = 1/Q_{4,\min}^{\text{exp}} = 2.500014(27)$. The measured spectrum also fixes the corresponding extension scale through Eq. (3). For the charged leptons,

$$r_*^\ell = \frac{R_2}{R_1} = 1.120\,42(7) \text{ GeV}^{1/2} \quad (25)$$

and therefore

$$m_*^\ell = (r_*^\ell)^2 = \left(\frac{m_e + m_\mu + m_\tau}{\sqrt{m_e} + \sqrt{m_\mu} + \sqrt{m_\tau}} \right)^2 = 1.255\,34(16) \text{ GeV}, \quad (26)$$

using PDG 2024 lepton masses [3]. If one substitutes the idealized value $Q_\ell^K = 2/3$ for Q_ℓ^{exp} in the closed-form identity $m^* = Q_0(m_e + m_\mu + m_\tau)$, while keeping the same measured mass sum $R_2 = m_e + m_\mu + m_\tau$, one obtains the corresponding idealized extension scale

$$m_*^{\ell,K} = Q_\ell^K(m_e + m_\mu + m_\tau) = \frac{2}{3}(m_e + m_\mu + m_\tau) = 1.255\,35(14) \text{ GeV}. \quad (27)$$

Here $m^* = (R_2/R_1)^2 = Q_0 R_2$ is the same identity as in the main text; the only knob being turned is Q_0 , no independent assumption on the lepton spectrum is added. This is numerically almost identical to m_*^ℓ , the small residual difference simply reflecting $Q_\ell^K - Q_\ell^{\text{exp}}$. The PDG 2024 reference $\overline{\text{MS}}$ charm mass $m_c(m_c) = 1.273(9) \text{ GeV}$ is 1.41% above m_*^ℓ .

The full dependence of $Q(e, \mu, \tau, x)$ on the fourth mass is shown in Fig. 1. The curve exhibits the unique minimum at $x = m_*^\ell$, the stronger lepton-data-specific lower bound $Q \geq Q_{4,\min}^{\text{exp}}$, and the proximity of the charm mass to that minimum. No other Standard Model particle mass falls within several percent of m_*^ℓ : the nearest are $m_\tau = 1.777 \text{ GeV}$ (41% above) and the b quark ($\times 3.3$ too heavy).

Because $Q_4(x)$ is stationary at $x = m_*^\ell$, its leading variation is quadratic in $(\sqrt{x} - \sqrt{m_*^\ell})$ near the minimum. Writing $r = \sqrt{x} = r_*^\ell + \epsilon$ and using $Q'(r_*^\ell) = 2R_1/(R_1 + r_*^\ell)^3$ from Eq. (5), one finds

$$Q_4(r) = Q_{4,\min}^{\text{exp}} + \frac{R_1 \epsilon^2}{(R_1 + r_*^\ell)^3} + O(\epsilon^3). \quad (28)$$

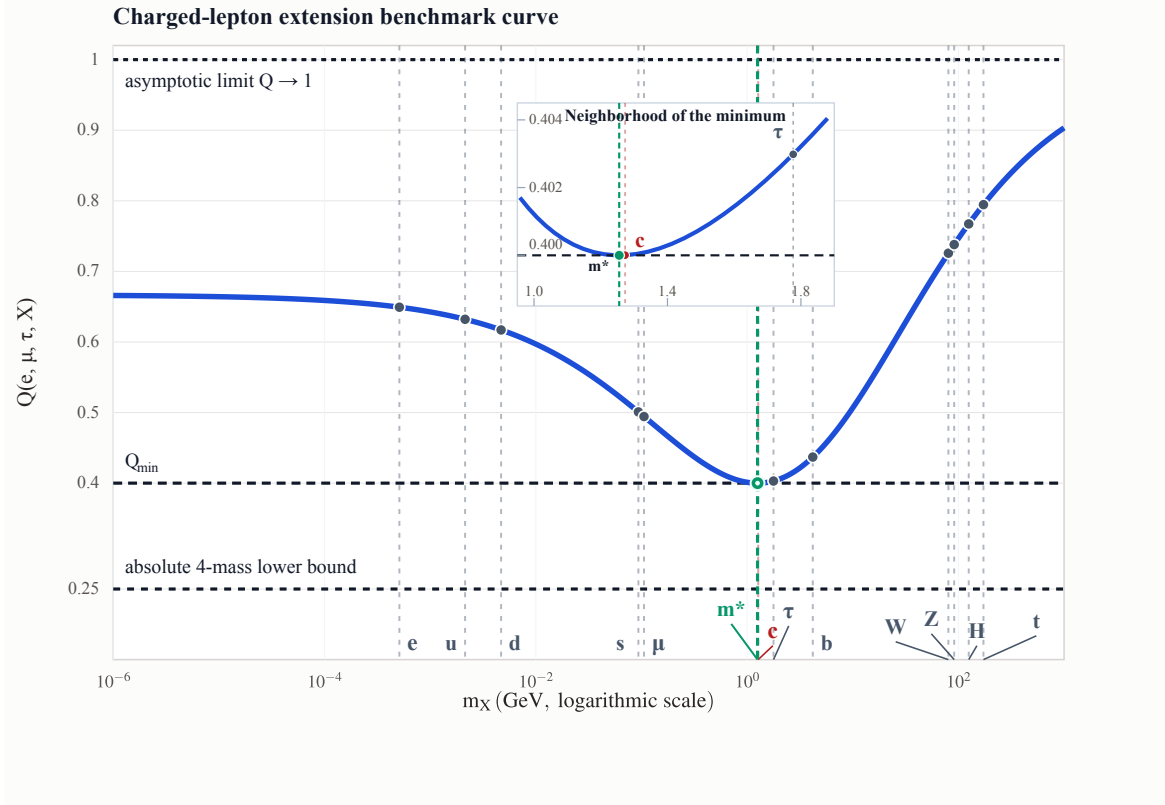


FIG. 1. Extended Koide ratio $Q(e, \mu, \tau, x)$ as a function of a hypothetical fourth mass x . The unique minimum occurs at the theorem-selected mass $m_*^\ell = 1.25534(16)$ GeV, while the physical charm mass lies nearby and gives $Q(e, \mu, \tau, c)$ close to the measured-input minimum $Q_{4,\min}^{\text{exp}}$; it is also close to $2/5$, which is the idealized target obtained in the limit $Q_\ell = 2/3$. The horizontal lines show the generic four-body lower bound $1/4$, the measured-input minimum $Q_{4,\min}^{\text{exp}}$, the idealized four-body minimum $2/5$, and the asymptotic upper limit $Q \rightarrow 1$. Standard Model mass markers are shown for orientation. The inset resolves the charm-scale neighborhood of the minimum. In the Lorentzian coordinate of Sec. III, the charm point sits at $u_c = +0.0034(17)$, i.e. essentially at the peak center.

Thus a fractional offset $\delta = (m_c - m_*^\ell)/m_*^\ell = 0.0141$ in the mass contributes only a few parts in 10^6 to Q . Direct evaluation gives

$$Q(e, \mu, \tau, c) = 0.4000025(64) \quad (29)$$

using $m_c(m_c) = 1.273(9)$ GeV. This corresponds to a relative deviation of 6.2 ppm from $Q_{4,\min}^{\text{K}} = 2/5$, and an 11.7 ppm relative deviation from the measured-input minimum $Q_{4,\min}^{\text{exp}}$. The latter is the direct benchmark selected by the theorem for the observed lepton inputs,

TABLE I. Lorentzian-coordinate values u_X for one-particle extensions of the charged-lepton base (e, μ, τ) , using the definition in Eq. (21). The quoted uncertainties are propagated from the input mass uncertainties.

Extender X	u_X
u	$-0.7616(56)$
d	$-0.7367(25)$
s	$-0.5024(85)$
c	$+0.0034(17)$
b	$+0.3040(9)$
W	$+0.90251(3)$
Z	$+0.91926(2)$
H	$+0.95824(11)$
t	$+0.99322(62)$

while the former is the corresponding ideal-Koide limit. In the Lorentzian coordinate of Sec. III, the same point corresponds to $u_c = +0.0034(17)$, i.e. essentially the center of the exact profile. In this sense, the charm mass provides a numerically close Standard Model realization of the theorem-selected minimizing point, although the theorem itself does not identify a physical SM state. Here the mass prescription is again intentionally pragmatic rather than derived: the charged leptons are kept at their pole masses because the observed Koide relation is formulated for those inputs, while charm is taken as the standard short-distance quantity $m_c(m_c)$ because the charm pole mass is less clean conceptually and numerically.

The observed extenders map to the Lorentzian coordinate values shown in Table I. Charm lies essentially at the peak center, whereas the electroweak and top masses all lie near the $u \sim 1$ shoulder where the Lorentzian has already fallen to about half height.

Within the Standard Model spectrum, the charm quark is the only particle lying comparably close to this minimizing scale, even though it is not the best-ranked entry in the broader scan of Sec. VII. A useful sanity check is the one-body problem $Q(m, X)$: because $Q(m) = 1$ for any single positive mass, the theorem reduces to the trivial statement that the minimizing extension recycles the original mass and gives $Q_{\min} = 1/2$. This serves only

as a control showing that scheme-expanded proximity is cheap to obtain in the trivial case; what makes the higher-body examples interesting is that they select nontrivial new scales rather than merely recycling the original one.

V. RENORMALIZATION-SCHEME SENSITIVITY

The extended formula (29) depends critically on the renormalization scheme used for m_c . This scheme sensitivity can be turned into a diagnostic. Table II shows $Q(e, \mu, \tau, c)$ for four natural choices of m_c .

The $\overline{\text{MS}}$ mass evaluated at its own mass scale is the conventional choice in Table II that lies closest to the measured-input minimum $Q_{4,\text{min}}^{\text{exp}}$. The pole mass, which deviates by 5,013 ppm from $Q_{4,\text{min}}^{\text{exp}}$, is disfavoured compared with the own-scale $\overline{\text{MS}}$ choice. This is best read as a scheme-sensitivity diagnostic, not as a derivation of a unique physical prescription: within this limited comparison, the closest conventional realization happens to occur for the own-scale $\overline{\text{MS}}$ charm mass.

The lepton masses, which enter as pole masses (the unique scheme-independent definition for stable particles), are unambiguous. For charm, by contrast, a short-distance mass is more appropriate than a pole mass, and the use of $m_c(m_c)$ is consistent with standard heavy-quark phenomenology [3]. This gives a limited physical rationale for the hybrid input set used here, but it does not elevate the result to a common-scheme or field-theoretic mass relation. A more uniform comparison, for example using running fermion masses or Yukawa couplings at a common high scale, would be a different question from the one addressed here; in particular, the known running-mass versions of the charged-lepton relation are already less sharp than the pole-mass formula [9]. We therefore do not reinterpret the present comparison as a common-scale running-mass test. While no renormalization scale makes a quark mass directly analogous to the charged-lepton pole masses, the standard short-distance quantity $m_c(m_c)$ is the least arbitrary low-energy benchmark for charm, because it is defined at the charm threshold and minimizes large perturbative logarithms; we therefore use it only as a pragmatic comparison convention, not as a common-scheme statement. The explicit M_Z exercise below is an external literature-based cross-check using the running masses quoted in Ref. [16]; it is not part of the scan pipeline of Sec. VII. The discrete scale set $\mu \in \{2 \text{ GeV}, m_c, m_b, m_Z, m_t\}$ is chosen simply to span the standard low-scale reference point,

TABLE II. Extended Koide ratio $Q(e, \mu, \tau, c)$ as a function of the charm mass scheme. Lepton pole masses are fixed throughout. The fourth column gives the corresponding Lorentzian mismatch coordinate u_c from Eq. (21) with propagated uncertainty. The m_c and Q entries carry 1σ uncertainties; the ppm column uses central values only and is included purely as a ranking diagnostic. Note in particular that for the $\mu = m_Z$ row the propagated 1σ band on the ppm entry is itself of order 10^4 ppm (driven by the $\delta m_c(M_Z) \approx 84$ MeV input uncertainty), so its ordering relative to the 2 GeV and pole-mass rows is not sharply established by the central values alone.

Scheme	m_c (GeV)	$(m_c - m_*^\ell)/m_*^\ell$	u_c	Q	relative ppm from $Q_{4,\min}^{\text{exp}}$
$\overline{\text{MS}}$ at $\mu = m_c$	1.273(9)	+1.41%	+0.0034(17)	0.400 002 5(64)	+12
$\overline{\text{MS}}$ at $\mu = 2$ GeV	1.094(8)	-12.86%	-0.0335(17)	0.400 445(46)	+1,119
$\overline{\text{MS}}$ at $\mu = m_Z$	0.619(84)	-50.69%	-0.166(30)	0.4110(40)	+27,429
Pole mass	1.67(5)	+33.03%	+0.0708(75)	0.40200(43)	+5,013

the heavy-quark thresholds, and one electroweak benchmark without introducing a denser a posteriori scale scan. The qualitative conclusion is stable across this set: the own-scale short-distance charm mass is the closest low-energy conventional choice, while the proximity does not survive as a common-scale statement.

The same ordering is visible in the Lorentzian coordinate: the own-scale $\overline{\text{MS}}$ choice has $|u_c| \ll 1$, while the alternative charm prescriptions move to visibly larger mismatches on the same exact kinematic profile. For the m_Z row, the much larger u_c error simply tracks the quoted uncertainty on the external running-mass benchmark $m_c(M_Z) = 0.619(84)$ GeV used below.

If the one-particle minimizer is applied once more to the measured lepton-plus-charm system, the preferred fifth mass returns to the same neighborhood: one finds $m_{*,5}^{\ell+c} = 1.2624(36)$ GeV (propagated from δm_τ and δm_c), only 0.86% below the reference $m_c(m_c) = 1.273(9)$ GeV, i.e. by $m_c - m_{*,5}^{\ell+c} = 10.6 \pm 9.7$ MeV when the uncertainties on both inputs are combined in quadrature. The two quantities are therefore statistically compatible at about the 1.1σ level rather than sharply distinguishable. In that limited sense the recursive continuation returns to the same charm-scale neighborhood rather than selecting a clearly new Standard Model mass scale.

For orientation, one may nonetheless inspect the common-scale running version at $\mu =$

M_Z . Using the published running masses of quarks and charged leptons in Ref. [16], one finds

$$Q_\ell(M_Z) = Q(e, \mu, \tau; M_Z) = 0.667\,928\,7(11) \quad (30)$$

and

$$m_*^\ell(M_Z) = 1.235\,30(15) \text{ GeV} , \quad Q_{4,\min}(M_Z) = \frac{Q_\ell(M_Z)}{1 + Q_\ell(M_Z)} = 0.400\,454\,0(40) . \quad (31)$$

The corresponding charm extension gives

$$Q(e, \mu, \tau, c; M_Z) = 0.41098(39) , \quad (32)$$

which lies about $2.63(98) \times 10^4$ ppm above the theorem-selected four-body minimum. Equivalently, $m_c(M_Z) = 0.619(84) \text{ GeV}$ lies about $49.9(6.8)\%$ below $m_*^\ell(M_Z)$. This common-scale benchmark therefore confirms, in line with the running-mass discussion of Ref. [9], that the sharp low-energy coincidence does not survive as a comparable M_Z statement.

The size of this M_Z shift can be understood from the QED running of the lepton masses themselves. At one-loop QED, all three charged leptons share the same mass anomalous dimension $\gamma_m^{(\text{QED})} = (3/2\pi) \alpha_{\text{em}}(\mu)$, because they carry the same electric charge. Their masses therefore run by a common multiplicative factor, $m_i(\mu) = R(\mu) m_i(\mu_0)$ for $i \in \{e, \mu, \tau\}$ with $R(\mu) = \exp[-\int_{\mu_0}^{\mu} \gamma_m^{(\text{QED})}(\mu') d \ln \mu']$. Because R is flavor-universal, $R_2(\mu) = R(\mu)^2 R_2$ and $R_1(\mu) = R(\mu) R_1$, so

$$Q_\ell(\mu) = \frac{R_2(\mu)}{R_1(\mu)^2} = Q_\ell , \quad m_*^\ell(\mu) = R(\mu)^2 m_*^\ell . \quad (33)$$

The Koide ratio is thus exactly RG-invariant at one-loop QED, and the entire continuous flow of the lepton-extension scale collapses to a single intensive trajectory governed by $R(\mu)$. With one-loop QED running and threshold-matched $\alpha_{\text{em}}(\mu)$ anchored at $\alpha_{\text{em}}^{-1}(M_Z) = 127.952$, $m_*^\ell(\mu)$ varies monotonically from 1.255 GeV at $\mu = 1 \text{ GeV}$ to 1.213 GeV at $\mu = 10 \text{ TeV}$, a 3% excursion over four decades, and crosses no Standard Model mass within that range. The $\sim 1.9 \times 10^{-3}$ shift in Q_ℓ between its low-scale value and the M_Z figure of Eq. (5.21) is therefore a subleading effect (higher-loop QED, weak corrections, and pole-to- $\overline{\text{MS}}$ scheme conversion in the inputs of Ref. [16]), not a leading-order running of Q_ℓ itself. Within the universal one-loop QED regime the discrete five-scale scan of Sec. VII reduces to repeated samples of this single curve.

VI. FOOT-ANGLE INTERPRETATION

Following Foot's geometric reformulation [4], let $r = (\sqrt{m_1}, \dots, \sqrt{m_N})$ and define θ_N as the angle between r and the democratic direction $\mathbf{1} = (1, \dots, 1)$. In model classes where the charged-lepton spectrum is generated from family-space bilinears or aligned vacuum expectation values, the mass amplitudes $r_i = \sqrt{m_i}$ can be more natural flavor coordinates than the masses m_i themselves; various family-space mechanisms along these lines have been proposed [17–19], but no unique derivation of this viewpoint is presently established. Then

$$Q_N = \frac{\|r\|^2}{(\mathbf{1} \cdot r)^2} = \frac{1}{N \cos^2 \theta_N}. \quad (34)$$

Equivalently,

$$\theta_N = \arccos\left(\frac{1}{\sqrt{NQ_N}}\right). \quad (35)$$

Combining Eq. (34) with $N_{\text{eff}} \equiv 1/Q$ gives the exact dictionary

$$\cos^2 \theta_N = \frac{N_{\text{eff}}}{N}. \quad (36)$$

Along the one-particle extension line with base moments $R_1 = \sum_i r_i$ and $R_2 = \sum_i r_i^2$, this becomes

$$\theta_{N+1}(r) = \arccos\left(\frac{R_1 + r}{\sqrt{N+1}\sqrt{R_2 + r^2}}\right). \quad (37)$$

Using the Lorentzian form of Eq. (23), one therefore has

$$\cos^2 \theta_{N+1}(u) = \frac{N_{\text{eff}}(u)}{N+1} = \frac{N_{\text{eff,max}}}{(N+1)(1+u^2)} = \frac{\cos^2 \theta_*}{1+u^2}. \quad (38)$$

Equivalently,

$$\theta_{N+1}(u) = \arccos\left(\frac{\cos \theta_*}{\sqrt{1+u^2}}\right). \quad (39)$$

So the Foot-angle miss is quadratic near the optimum, $\theta_{N+1}(u) = \theta_* + u^2/(2 \tan \theta_*) + O(u^4)$, as expected at the center of an even Lorentzian profile. Thus Q is equivalently an angular misalignment variable: smaller Q means better alignment with the democratic direction. Propagating the quoted mass uncertainties through this relation gives for the observed charged leptons $\theta_\ell = 0.785\,393\,9(9) \text{ rad} = 44.999\,756(52)^\circ$, extremely close to the exact Koide angle $\pi/4$ [4]. Along the constrained extension line where the original mass amplitudes are held fixed, the theorem-selected value $r^* = R_2/R_1$ is precisely the point of least angular deviation from the democratic direction. Correspondingly,

$$\theta_* = \theta_{N+1}(r^*) = \arccos\left(\frac{1}{\sqrt{(N+1)Q_{N+1,\text{min}}}}\right) = \arccos\left(\sqrt{\frac{1+Q_0}{(N+1)Q_0}}\right). \quad (40)$$

The theorem-selected four-body minimum $Q_{4,\min}^{\text{exp}} = 0.399\,997\,8(43)$ corresponds to

$$\theta_* = 0.659\,054(7) \text{ rad} = 37.761\,04(40)^\circ. \quad (41)$$

The physical charm extension of Eq. (29), $Q(e, \mu, \tau, c) = 0.400\,002\,5(64)$, gives

$$\theta_c = 0.659\,062(10) \text{ rad} = 37.761\,48(59)^\circ. \quad (42)$$

The angular miss is therefore only

$$\Delta\theta_c = \theta_c - \theta_* = 0.000\,008(12) \text{ rad} = 0.000\,43(71)^\circ. \quad (43)$$

So the charm point is best viewed as a very small democratic-misalignment perturbation away from the exact theorem minimum. The uncertainty on $\Delta\theta_c$ is larger than its central value because it is obtained by subtracting two very close angles with independent propagated errors; that does not mean $r_c - r_*^\ell$ vanishes within error, only that the angular distinction is not by itself statistically sharp.

The angle θ_c is not, however, close to any especially simple rational multiple of π . For example, it lies $1.761\,48(59)^\circ$ above $\pi/5$. So what is distinctive here is not proximity to a simple standalone angle, but proximity to the theorem-selected democratic angle associated with the charged-lepton base itself.

VII. LOOK-ELSEWHERE CALIBRATION

To quantify where the charm continuation sits within the non-neutrino SM one-particle extensions, we performed an exhaustive scan of all distinct one-particle extensions of 2-body and 3-body seeds drawn from $\{e, \mu, \tau, u, d, s, c, b, t, W, Z, H\}$. The 2-/3-body restriction is a deliberate choice of comparison class: 1-body bases give the trivial $Q(m) = 1$ problem whose extension reduces to a single-mass match and adds no useful comparison value, while 4-body bases of distinct non-neutrino SM species yield only $\binom{12}{4} = 495$ patterns from which 8 extensions each can be drawn, a comparison class so small that it is dominated by the few clusters already containing the charged-lepton triplet and is not informative as a look-elsewhere sample. The 2-/3-body window is therefore the smallest non-trivial choice that gives both an interpretable rank and a sample size large enough to populate the low-miss tail. If a trial contains quarks, all quark masses in that trial are evaluated at the same

common $\overline{\text{MS}}$ scale chosen from $\mu \in \{2 \text{ GeV}, m_c, m_b, m_Z, m_t\}$. Purely non-quark trials are scale-independent and are evaluated once with pole masses for e, μ, τ, W, Z, H . The scan uses unordered bases with distinct species, giving 660 pair-base patterns and 1,980 triple-base patterns, for 2,640 collapsed physical patterns in total. The corresponding raw trial count is $120 + 5(2,640 - 120) = 12,720$: the 120 purely non-quark patterns appear once, while the remaining 2,520 quark-containing patterns are evaluated at five common scales. Here “common-scale” means common-scale for the quark masses within a given trial; the charged leptons and electroweak bosons remain at their usual reference masses (pole masses for e, μ, τ, W, Z, H) regardless of the quark scale, so the scan inherits the same mixed-definition convention that we labeled pragmatic for the standalone charm comparison. For the scan itself, the quark masses are generated from the PDG input values by one-loop QCD running with $\alpha_s(M_Z) = 0.1179$, using continuous matching of α_s and the running masses across the m_c, m_b , and m_t thresholds and changing the active flavor number stepwise at those thresholds. The seed inputs are the PDG 2024 short-distance values $m_q(m_q)$ for $q \in \{c, b, t\}$ and $m_q(2 \text{ GeV})$ for $q \in \{u, d, s\}$, run from their reference scales to each target μ in the grid; no pole-to- $\overline{\text{MS}}$ conversion is applied beyond what is implicit in the PDG input choice. This is the common-scale prescription used to generate the leaderboard tables below. It is distinct from the separate M_Z paragraph of Sec. V, which is an external literature cross-check based on the running masses quoted in Ref. [16] rather than a row taken from the scan pipeline itself. We ranked the trials by the relative miss from the measured-input theorem minimum,

$$\Delta_Q \equiv 10^6 \frac{|Q_{\text{ext}} - Q_{\text{min}}|}{Q_{\text{min}}}. \quad (44)$$

This gives a controlled benchmark ranking that avoids mixed-scale quark assignments within a single trial. The resulting raw and collapsed fractions are scan frequencies within this chosen benchmark set, not formal p-values derived from a probabilistic ensemble. Two further caveats apply to how the rank statistics should be read. First, the common-scale grid $\mu \in \{2 \text{ GeV}, m_c, m_b, m_Z, m_t\}$ contains $\mu = m_c$, which is precisely the scale at which the charged-lepton-plus-charm realization is closest to its theorem minimum; the grid therefore overlaps a scale that is favorable for the row of interest. Second, the collapse rule keeps the best-of-five common-scale realizations per physical pattern, which is itself a selection on the same ranking variable Δ_Q and favors patterns whose theorem-selected scale happens to align with one of the grid scales. The leaderboard rank of any specific row, including the

TABLE III. Benchmark-scan rank of the charged-lepton-plus-charm result in the common-scale scan. Here Δ_Q is the relative ppm miss from the theorem minimum. “Raw” counts each common-scale realization as a separate trial, while “collapsed” keeps only the sharpest common-scale realization for each physical species pattern (base, X).

Scan scope	Trials	Rank of $e, \mu, \tau \rightarrow c$	Fraction at or better
Raw all trials	12,720	33	0.259%
Raw 3-body bases only	9,660	30	0.311%
Collapsed all patterns	2,640	24	0.909%
Collapsed 3-body patterns only	1,980	21	1.061%

charged-lepton-plus-charm one, can therefore shift by several positions under nearby grid redefinitions; the rank statements below should be read as conditional on the specific grid and collapse rule adopted here, not as grid-independent quantities. Because the benchmark class is defined by the non-neutrino SM spectrum, one-particle extensions of 2-body and 3-body seeds, and the small conventional common scale set above, these fractions should be read only conditionally on that chosen ensemble. They are therefore benchmark ranks within a partly structured and partly a posteriori comparison class, not global measures of how surprising the charged-lepton-plus-charm continuation would be in a broader flavor-model space.

For the charged-lepton seed, the target row is $Q(e, \mu, \tau, c(m_c)) = 0.400\,002\,5$, which lies 11.7 ppm above the measured-input minimum $Q_{4,\min}^{\text{exp}} = 0.399\,997\,8$. Table III shows that this places the charm continuation near the low-miss end of the distribution, but not as a unique outlier: in the common-scale scan it is roughly a top-0.3% result in the raw trial set and about a top-1% result after collapsing repeated scale realizations to one physical pattern. Figure 2 displays the same picture graphically: the raw and collapsed Δ_Q distributions from the common-scale scan both place the charged-lepton-plus-charm entry (red reference line) in the low-miss tail, but within a broader population of similarly close near-minima rather than as a singular outlier. The best-ranked collapsed near-minima are dominated by electroweak/heavy-quark clusters such as $(\mu, b, H) \rightarrow Z$ and $(\tau, b, H) \rightarrow W$. The charm case therefore remains uncommon, but its status is empirical rather than statistically singular. The first 30 entries of the collapsed common-scale leaderboard are listed explicitly in

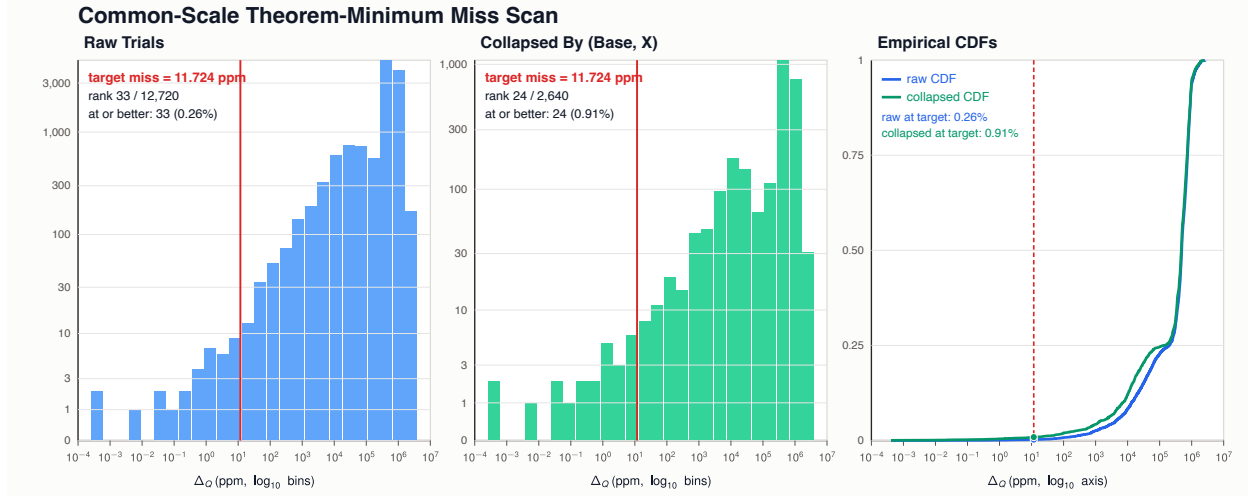


FIG. 2. Distribution of the relative miss $\Delta_Q = 10^6 |Q_{\text{ext}} - Q_{\text{min}}| / Q_{\text{min}}$ in the common-scale scan. The left and middle panels show the raw and collapsed trial sets; the right panel compares the raw and collapsed empirical CDFs. The red reference line indicates the charged-lepton-plus-charm result. The raw panel counts each common-scale realization separately, while the collapsed panel keeps only the best common-scale realization for each physical species pattern (base, X). The figure makes clear that the charm continuation lies near the low-miss end of the distribution, but within a broader population of electroweak/heavy-sector near-minima.

Appendix B, specifically in Table IV. Within that full collapsed leaderboard, the charged-lepton-plus-charm entry appears as row 24, marked with a star. It is worth reading that row against the rows immediately above it, since the better-ranked entries are mostly dense electroweak or heavy-quark clusters rather than comparably direct continuations of the charged-lepton Koide pattern. This electroweak/heavy-sector dominance is itself informative: once a base tuple already lies in the dense $W/Z/H/\text{top}$ region, nearby minima are often driven by local spectral clustering rather than by a continuation of an already distinguished flavor relation. Restricting the collapsed leaderboard to fermions only leaves 756 patterns, within which $e, \mu, \tau \rightarrow c$ ranks 6th (top 0.79%); the leading entries of that restricted ranking are listed in Appendix B, specifically in Table V. In that narrower comparison class the charm case remains one of the best-ranked fermionic continuations. Table IV also shows the low-scale $(e, \mu) \rightarrow s$ echo at row 7. That case is numerically sharp, but it is less interesting physically because the base pair $Q(e, \mu)$ is not tied to a comparably simple distinguished target. Its apparent closeness is driven by the specific low-scale choice for the strange-quark

mass, and, as in the charm comparison, the level of agreement changes under reasonable changes of scheme or scale. Numerically, the (e, μ) base has $Q(e, \mu) = 0.8784119487(12)$, the theorem selects $m_*^{e\mu} = 93.2604655(22)$ MeV and $Q_{3,\min}^{e\mu} = 0.46763541369(33)$, while the low-scale strange input $m_s(2 \text{ GeV}) = 93.4(9)$ MeV gives $Q(e, \mu, s) = 0.46763548(84)$, a central miss of 0.14 ppm with an uncertainty of 180 ppm. At current strange-mass precision this is therefore not a statistically informative sub-ppm coincidence; it is best regarded as a low-scale control example whose central value happens to sit very close to the theorem minimum. By contrast, the charm extension $Q(e, \mu, \tau, c) = 0.400\,002\,5(64)$ has a propagated relative uncertainty of about 16 ppm, of the same order as its 11.7 ppm central miss, so the charm coincidence is statistically informative at roughly the $\lesssim 1\sigma$ level rather than buried inside an order-of-magnitude larger error band as for $(e, \mu) \rightarrow s$. This is the key qualitative distinction in the scan: several patterns are close to their theorem minima, but $Q(e, \mu, \tau, c)$ is the clearest case in which the extension is numerically close *and* the unextended base $Q(e, \mu, \tau)$ is already very close to an interesting simple fraction, namely the Koide value $2/3$.

The same theorem can also serve as a mass estimator once a base tuple is regarded as physically meaningful but the extension mass is not yet known. That is the logic behind the charm application, and it is why the theorem may still be useful outside the charged-lepton case: if one had a credible Koide-like target for a neutrino sector or another hidden multiplet, the closed-form minimizer $m^* = (R_2/R_1)^2$ would immediately turn the known members into a predicted extension scale. In the present paper we do not push that logic for neutrinos, because any such target assignment is much more speculative than the charged-lepton Koide relation itself.

VIII. CONCLUSIONS

We have proved and applied the Q -minimum theorem: for any N -particle group with Koide ratio Q_0 , the minimum of Q over all extensions by a single additional mass is $Q_{\min} = Q_0/(1 + Q_0)$, achieved at the *optimal mass* $m^* = (R_2/R_1)^2$. In the associated effective-participant language, $N_{\text{eff}} \equiv 1/Q$, the one-particle theorem reads $N_{\text{eff,max}} = N_{\text{eff},0} + 1$, while the equal- k multiplet extension theorem reads $N_{\text{eff,max}}^{(k)} = N_{\text{eff},0} + k$.

The theorem itself is purely kinematic. It does not explain why any physical spectrum

should lie near the minimizing extension; rather, it defines a unique benchmark against which candidate continuations can be measured. The exact Lorentzian-coordinate reformulation developed in Sec. III should be read in the same spirit: it is an exact reparameterization of the kinematic extension curve, not a literal dynamical Breit–Wigner resonance. No global statistical significance is claimed for the charm proximity beyond its rank within the explicit benchmark ensemble defined in Sec. VII.

Applied to the charged leptons:

- The idealized value $Q_\ell^K = 2/3$ implies the exact four-body benchmark value $Q_{4,\min}^K = 2/5$. In the same idealized language this is $N_{\text{eff},0}^K = 3/2 \rightarrow N_{\text{eff,max}}^K = 5/2$.
- The measured lepton input gives the minimizing mass $m_*^\ell = 1.255\,34(16)$ GeV and the corresponding minimum $Q_{4,\min}^{\text{exp}} = 0.399\,997\,8(43)$. Equivalently, the measured seed and theorem-selected peak values are $N_{\text{eff},0}^{\text{exp}} = 1.500014(27)$ and $N_{\text{eff,max}}^{\text{exp}} = 2.500014(27)$.
- The conventional own-scale short-distance charm mass $m_c(m_c) = 1.273(9)$ GeV is 1.4% above m_*^ℓ , yielding $Q(e, \mu, \tau, c) = 0.400\,002\,5(64)$, which lies 11.7 ppm above $Q_{4,\min}^{\text{exp}}$ and, in the idealized Koide limit, 6.2 ppm above $Q_{4,\min}^K = 2/5$. In the exact Lorentzian coordinate it corresponds to $u_c = +0.0034(17)$, i.e. essentially the peak center.
- Among the conventional charm-mass choices considered here, $m_c(m_c)$ gives the closest realization within the low-energy comparison class used here. This comparison is intentionally mixed-definition: lepton pole masses are kept because that is the empirical charged-lepton Koide input, while charm is represented by the short-distance quantity $m_c(m_c)$ because a charm pole mass is not comparably clean. This gives a practical phenomenological convention, not a model-derived common scheme; when all four masses are instead moved to the common scale M_Z , one finds $Q(e, \mu, \tau, c; M_Z) = 0.41098(39)$, about $2.63(98) \times 10^4$ ppm above the theorem-selected minimum, so the low-energy charm proximity does not survive as a common-scale statement.
- In Foot’s angular language, the near-45° lepton geometry is the classic observation of Ref. [4], while the new point here is that the theorem selects the least-misaligned continuation angle $\theta_* = 0.659\,054(7)$ rad = 37.761 04(40)° and that the physical charm extension lands at $\theta_c = 0.659\,062(10)$ rad = 37.761 48(59)°, i.e. only $\Delta\theta_c =$

0.000 008(12) rad = 0.000 43(71) $^\circ$ away from that theorem-selected democratic direction.

- In a common-scale look-elsewhere scan over all non-neutrino SM 2-body and 3-body bases, the charged-lepton-plus-charm pattern ranks 33/12,720 in the raw trial set and 24/2,640 after collapsing repeated common-scale realizations, so it lies near the low-miss end of the distribution but is not unique. Restricting to fermion-only collapsed patterns moves it to rank 6/756. The full collapsed scan also contains a numerically sharper low-scale $(e, \mu) \rightarrow s$ echo, but it is less structurally compelling because it starts from the nondistinguished two-body value $Q(e, \mu)$ and its closeness is more convention-dependent.

The Q -minimum theorem itself is exact. Its phenomenological application to the charm quark remains empirical: the theorem identifies a minimizing mass scale, and the physical charm mass lies close to it in one practical mixed-definition convention. The exhaustive 2-body and 3-body scan shows that this proximity is uncommon but not unique once the nearby Standard Model alternatives are enumerated in a controlled quark-common-scale benchmark setup. That is the main claim of the paper: not that the theorem explains flavor, but that it defines a benchmark and that the charged-lepton-plus-charm continuation lands high in the resulting Standard Model ranking, especially within the narrower fermion-only comparison class. Those rank statements are conditional on the benchmark class chosen here and should not be reinterpreted as global p-values or prior probabilities for flavor structure.

Within the broader Koide literature, the principal new results of this work are the exact one-particle minimization theorem itself, its closed-form extension rule $Q_{\min} = Q_0/(1 + Q_0)$ with minimizer $m^* = (R_2/R_1)^2$, its equal-multiplet extension $Q_{\min}^{(k)} = Q_0/(1 + kQ_0)$ with all added amplitudes fixed at the same $r^* = R_2/R_1$ (in particular, the classic Koide value $Q_0 = 2/3$ gives the exact one-particle minimum $Q_{\min} = 2/5$), its effective-participant reformulation $N_{\text{eff,max}} = N_{\text{eff},0} + 1$ and $N_{\text{eff,max}}^{(k)} = N_{\text{eff},0} + k$, the exact Lorentzian coordinate form of the one-particle extension curve, and the corresponding Standard Model calibration, including the explicit charged-lepton-plus-charm benchmark $Q(e, \mu, \tau, c) = 0.400\,002\,5(64)$ together with its scan-based context. Those results do not supply a dynamical flavor model, but they do define a reproducible benchmark that may be useful in future work on Koide-inspired extensions or hidden-sector multiplets. The limited outlook is therefore simply

this: whenever a base multiplet is independently motivated, the theorem supplies a unique continuation scale against which any candidate additional state can be compared. Whether that benchmark has deeper dynamical meaning is a separate question not pursued here.

ACKNOWLEDGMENTS

The author thanks Christian Schmidt for valuable correspondence and the Particle Data Group for maintaining the data compilations used throughout this work.

Appendix A: Explicit r -space computation of the measured-input minimum

Using PDG 2024 lepton masses (in MeV),

$$m_e = 0.51099895000(15), \quad (\text{A1})$$

$$m_\mu = 105.6583755(23), \quad (\text{A2})$$

$$m_\tau = 1776.86(21). \quad (\text{A3})$$

The corresponding mass amplitudes are

$$r_e = \sqrt{m_e} = 0.71484190560(11) \text{ MeV}^{1/2}, \quad (\text{A4})$$

$$r_\mu = \sqrt{m_\mu} = 10.27902600(11) \text{ MeV}^{1/2}, \quad (\text{A5})$$

$$r_\tau = \sqrt{m_\tau} = 42.1528(25) \text{ MeV}^{1/2}. \quad (\text{A6})$$

Hence

$$R_1 = r_e + r_\mu + r_\tau = 53.1467(25) \text{ MeV}^{1/2}, \quad (\text{A7})$$

$$R_2 = r_e^2 + r_\mu^2 + r_\tau^2 = m_e + m_\mu + m_\tau = 1883.029(210) \text{ MeV}, \quad (\text{A8})$$

$$Q_\ell^{\text{exp}} = \frac{R_2}{R_1^2} = \frac{1883.029}{2824.572} = 0.666\,661(12), \quad (\text{A9})$$

$$r^* = \frac{R_2}{R_1} = \frac{1883.029}{53.1467} = 35.4308(23) \text{ MeV}^{1/2}, \quad (\text{A10})$$

$$m_*^\ell = (r^*)^2 = 1255.34(16) \text{ MeV} = 1.25534(16) \text{ GeV}. \quad (\text{A11})$$

The relative uncertainty on R_2 is $\delta R_2/R_2 \approx 1.1 \times 10^{-4}$, inherited essentially entirely from $\delta m_\tau/m_\tau \approx 1.2 \times 10^{-4}$, because m_τ dominates the sum. The smaller relative uncertainty on

Q_ℓ^{exp} ($\approx 1.8 \times 10^{-5}$) and on $Q_{4,\text{min}}^{\text{exp}}$ ($\approx 1.1 \times 10^{-5}$) reflects partial cancellation: $Q = R_2/R_1^2$ depends on m_τ both through $R_2 \propto m_\tau$ and through $R_1 \propto \sqrt{m_\tau}$, so $\partial \ln Q / \partial \ln m_\tau = m_\tau / R_2 - r_\tau / R_1 \approx 0.943 - 0.793 = 0.150$, suppressing the propagated Q error by roughly an order of magnitude relative to the input. The further suppression on $Q_{4,\text{min}} = Q_\ell / (1 + Q_\ell)$ is the kinematic factor $\partial Q_{4,\text{min}} / \partial Q_\ell = 1 / (1 + Q_\ell)^2 \approx 0.36$. The theorem then gives

$$Q_{4,\text{min}}^{\text{exp}} = \frac{Q_\ell^{\text{exp}}}{1 + Q_\ell^{\text{exp}}} = \frac{0.666\,661}{1.666\,661} = 0.399\,997\,8(43). \quad (\text{A12})$$

Direct evaluation of the charm extension with $m_c = 1273(9) \text{ MeV}$ and $r_c = \sqrt{m_c} = \sqrt{1273 \text{ MeV}} = 35.679(126) \text{ MeV}^{1/2}$ gives

$$R'_1 = R_1 + r_c = 88.8258(126) \text{ MeV}^{1/2}, \quad (\text{A13})$$

$$R'_2 = R_2 + r_c^2 = 3156.0(9.0) \text{ MeV}, \quad (\text{A14})$$

$$Q_4 = \frac{R'_2}{(R'_1)^2} = \frac{3156.029}{7889.998} = 0.400\,002\,5(64). \quad (\text{A15})$$

The corresponding measured effective-participant values and Lorentzian coordinate are

$$N_{\text{eff},0}^{\text{exp}} = \frac{1}{Q_\ell^{\text{exp}}} = 1.500\,014(27), \quad (\text{A16})$$

$$N_{\text{eff},\text{max}}^{\text{exp}} = \frac{1}{Q_{4,\text{min}}^{\text{exp}}} = 2.500\,014(27), \quad (\text{A17})$$

$$u_c = \frac{p_c - Q_{4,\text{min}}^{\text{exp}}}{\sqrt{Q_{4,\text{min}}^{\text{exp}}(1 - Q_{4,\text{min}}^{\text{exp}})}} = +0.0034(17), \quad (\text{A18})$$

where $p_c = r_c / (R_1 + r_c) = 0.40168(85)$ is the normalized amplitude share of the charm extender. This is the measured-input realization of the exact identity $N_{\text{eff},\text{max}} = N_{\text{eff},0} + 1$ discussed in the main text. The uncertainty on R'_2 is dominated by δm_c , whereas the uncertainty on Q_4 is much smaller because the charm input lies close to the minimizing point, where the first derivative vanishes. The residuals are

$$\frac{Q_4 - 2/5}{2/5} = 6.18 \times 10^{-6} \quad (6.2 \text{ ppm}), \quad (\text{A19})$$

$$\frac{Q_4 - Q_{4,\text{min}}^{\text{exp}}}{Q_{4,\text{min}}^{\text{exp}}} = 1.17 \times 10^{-5} \quad (11.7 \text{ ppm}). \quad (\text{A20})$$

Appendix B: Collapsed common-scale look-elsewhere leaderboard

Table IV lists the first 30 entries of the collapsed common-scale leaderboard discussed in Sec. VII. Here “collapsed” means that for each physical species pattern (base, X) we keep

only the common-scale realization with the smallest relative ppm miss from the theorem minimum. In the tables below, m^* is the theorem-selected extension mass, m_X is the actual mass of the candidate extender X at the listed scale, $\delta_m \equiv 10^6(m_X - m^*)/m^*$ is their signed relative offset in ppm, u_{obs} is the Lorentzian-coordinate value of the observed extender defined in Eq. (21), and $\Delta\theta \equiv \theta_{\text{obs}} - \theta_*$ is the corresponding Foot-angle miss, quoted in μrad .

Table V shows the top entries of the collapsed leaderboard after removing W , Z , and H and restricting to the fermionic species $\{e, \mu, \tau, u, d, s, c, b, t\}$. In that reduced comparison class the charged-lepton-plus-charm target moves from row 24 in the full table to row 6.

TABLE IV. First 30 entries of the collapsed common-scale leaderboard, ranked by $\Delta_Q \equiv 10^6 |Q_{\text{obs}} - Q_{\text{min}}|/Q_{\text{min}}$. The mass columns m^* and m_X are in GeV. The angle columns θ_* and θ_{obs} are in rad, while the final column gives the Foot-angle miss $\Delta\theta$ in μrad . The signed mass-offset column is $\delta_m \equiv 10^6(m_X - m^*)/m^*$, and the u_{obs} column is the Lorentzian-coordinate value from Eq. (21) with propagated 1σ uncertainty. A star marks the charged-lepton-plus-charm target row. The scale column lists the common quark evaluation scale; “indep.” denotes a pure non-quark pattern. Several entries in this table have $|u_{\text{obs}}| \gtrsim 0.3$, well outside the small-deviation regime where the Lorentzian profile of Eq. (23) retains its peak character; the listed u_{obs} values for those rows should be read as positions on the exact kinematic curve rather than as “near-peak” realizations.

Rank	Pattern	Scale	Q_{min}	Q_{obs}	Δ_Q	m^*	m_X	δ_m	u_{obs}	θ_*	θ_{obs}	$\Delta\theta$
1	$\mu, b, H \rightarrow Z$	m_b	0.413238900	0.413238900	0.000411	91.195134	91.187621	-82.381	-0.00013(25)	0.67963(16)	0.67963(16)	0.0003(65)
2	$\tau, b, H \rightarrow W$	2 GeV	0.379081210	0.379081210	0.000487	80.376505	80.369193	-90.969	-0.00218(26)	0.62307(19)	0.62307(19)	0.0003(80)
3	$\mu, s, Z \rightarrow W$	m_c	0.467992686	0.467992689	0.007778	80.397609	80.369193	-353.438	-0.00066(8)	0.75118(55)	0.75118(55)	0.004(45)
4	$t, W \rightarrow H$	m_t	0.340010524	0.340010532	0.022759	125.120300	125.200015	+637.106	-0.01056(42)	0.1406(19)	0.1406(19)	0.1(19)
5	$\mu, b, t \rightarrow H$	m_t	0.430746950	0.430746960	0.023921	125.278251	125.200015	-624.492	-0.00933(59)	0.70466(42)	0.70466(42)	0.01(50)
6	$\tau, c, H \rightarrow Z$	m_t	0.416276923	0.416276958	0.084543	91.080115	91.187621	+1180.344	+0.00789(25)	0.68415(16)	0.68415(16)	0.052(95)
7	$e, \mu \rightarrow s$	2 GeV	0.467635414	0.467635479	0.139122	0.093260	0.093400	+1496.181	+0.00037(249)	0.56557910660(56)	0.5655792(94)	0.1(94)
8	$\mu, t, W \rightarrow H$	m_Z	0.334326147	0.334326255	0.324022	125.502579	125.200015	-2410.815	-0.00385(42)	0.52617(54)	0.52617(54)	0.3(18)
9	$e, t, W \rightarrow H$	m_t	0.339544132	0.339544272	0.413088	124.860701	125.200015	+2717.541	-0.01008(42)	0.53930(46)	0.53930(45)	0.3(19)
10	$b, W, H \rightarrow Z$	m_t	0.303543312	0.303543491	0.590759	90.883361	91.187621	+3347.813	+0.00479(14)	0.43344(18)	0.43344(18)	0.64(25)
11	$s, c, b \rightarrow \tau$	m_t	0.320350290	0.320350572	0.881519	1.769727	1.776860	+4030.952	-0.08043(43)	0.4877(30)	0.4877(30)	0.8(21)
12	$u, t, W \rightarrow H$	m_t	0.339249104	0.339249413	0.909015	124.696947	125.200015	+4034.329	-0.00957(44)	0.53857(50)	0.53857(50)	0.8(29)
13	$s, b, H \rightarrow Z$	m_b	0.414487581	0.414488224	1.552190	91.650117	91.187621	-5046.319	-0.00079(26)	0.68212(50)	0.68212(50)	0.96(63)
14	$\mu, t, Z \rightarrow H$	m_t	0.331521875	0.331522390	1.553503	125.865037	125.200015	-5283.608	-0.01141(40)	0.51885(45)	0.51886(45)	1.4(37)
15	$d, t, W \rightarrow H$	m_t	0.338892548	0.338893146	1.764836	124.499519	125.200015	+5626.496	-0.00911(42)	0.53769(47)	0.53769(47)	1.5(40)
16	$c, t, Z \rightarrow H$	m_Z	0.322297431	0.322298345	2.837812	124.301269	125.200015	+7230.387	+0.00261(41)	0.49340(61)	0.49340(60)	2.6(55)
17	$\mu, c, b \rightarrow \tau$	m_Z	0.311380167	0.311381062	2.875405	1.789931	1.776860	-7302.211	-0.07882(41)	0.46004(68)	0.46004(69)	2.9(28)
18	$s, t, W \rightarrow H$	m_Z	0.335827143	0.335828648	4.484159	126.328634	125.200015	-8933.987	-0.00424(42)	0.53001(66)	0.53001(66)	3.8(66)
19	$e, \tau, s \rightarrow c$	m_c	0.401297789	0.401300569	6.928563	1.259408	1.273000	+10792.368	+0.00092(53)	0.6611(34)	0.6611(34)	4.5(74)
20	$s, b, t \rightarrow H$	m_t	0.433408931	0.433412261	7.683021	126.609018	125.200015	-11128.773	-0.00992(59)	0.70827(53)	0.70827(53)	4.5(89)
21	$s, t, Z \rightarrow H$	m_t	0.333094273	0.333097021	8.249893	126.736889	125.200015	-12126.487	-0.01178(40)	0.52298(58)	0.52298(59)	7.2(85)
22	$\mu, \tau \rightarrow c$	m_c	0.406449527	0.406453397	9.520976	1.289105	1.273000	-12493.044	-0.00309(49)	0.4380058(60)	0.438016(13)	10(11)
23	$c, b, H \rightarrow W$	m_c	0.382528794	0.382533207	11.534316	81.501266	80.369193	-13890.251	-0.00719(26)	0.62933(28)	0.62934(28)	7.9(13)
24*	$e, \mu, \tau \rightarrow c$	m_c	0.399997781	0.400002471	11.723747	1.255341	1.273000	+14066.729	+0.0034(17)	0.6590545(40)	0.6590620(86)	7.6(77)
25	$\tau, s \rightarrow c$	m_c	0.407781159	0.407787380	15.256796	1.293413	1.273000	-15782.573	-0.00567(54)	0.4415(56)	0.4415(56)	16(18)
26	$\mu, u \rightarrow s$	m_b	0.441384763	0.441392989	18.635453	0.085012	0.083546	-17245.942	+0.02575(583)	0.5176(10)	0.5176(10)	16(120)
27	$\tau, c, t \rightarrow H$	m_Z	0.425827919	0.425836775	20.797273	127.532475	125.200015	-18289.142	-0.00298(60)	0.69786(46)	0.69787(48)	12(15)
28	$d, b, H \rightarrow Z$	m_c	0.416316467	0.416325516	21.734841	92.930262	91.187621	-18752.132	-0.00917(25)	0.68420(21)	0.68422(21)	13(15)
29	$\tau, W, H \rightarrow Z$	indep.	0.309913954	0.309921197	23.369713	93.118011	91.187621	-20730.574	-0.00490(14)	0.45525(53)	0.45527(54)	24(14)
30	$\mu, \tau, d \rightarrow c$	2 GeV	0.387706554	0.387716195	24.866871	1.194975	1.170735	-20284.763	+0.01546(52)	0.63848(100)	0.63849(100)	17(12)

TABLE V. Top 10 entries of the fermion-only collapsed leaderboard (756 patterns total), obtained by restricting the scan to $\{e, \mu, \tau, u, d, s, c, b, t\}$. The mass columns m^* and m_X are in GeV. The angle columns θ_* and θ_{obs} are in rad, while the final column gives the Foot-angle miss $\Delta\theta$ in μrad ; all three angle columns use 1σ uncertainties in APS-style parenthetical notation. The signed mass-offset column is $\delta_m \equiv 10^6(m_X - m^*)/m^*$, and the u_{obs} column is the Lorentzian-coordinate value from Eq. (21). For the charged-lepton-plus-charm target row, $\Delta\theta = 7.6(77)\mu\text{rad}$. A star marks the charged-lepton-plus-charm target row.

Rank	Pattern	Scale	Q_{min}	Q_{obs}	Δ_Q	m^*	m_X	δ_m	u_{obs}	θ_*	θ_{obs}	$\Delta\theta$
1	$e, \mu \rightarrow s$	2 GeV	0.467635414	0.467635479	0.139122	0.093260	0.093400	+1496.181	+0.00037(249)	0.56557910660(56)	0.5655792(94)	0.1(94)
2	$s, c, b \rightarrow \tau$	m_t	0.320350290	0.320350572	0.881519	1.769727	1.776860	+4030.952	-0.08043(43)	0.4877(30)	0.4877(30)	0.8(21)
3	$\mu, c, b \rightarrow \tau$	m_Z	0.311380167	0.311381062	2.875405	1.789931	1.776860	-7302.211	-0.07882(41)	0.46004(68)	0.46004(69)	2.9(28)
4	$e, \tau, s \rightarrow c$	m_c	0.401297789	0.401300569	6.928563	1.259408	1.273000	+10792.368	+0.00092(53)	0.6611(34)	0.6611(34)	4.5(74)
5	$\mu, \tau \rightarrow c$	m_c	0.406449527	0.406453397	9.520976	1.289105	1.273000	-12493.044	-0.00309(49)	0.4380058(60)	0.438016(13)	10(11)
6*	$e, \mu, \tau \rightarrow c$	m_c	0.399997781	0.400002471	11.723747	1.255341	1.273000	+14066.729	+0.0034(17)	0.6590545(40)	0.6590620(86)	7.6(77)
7	$\tau, s \rightarrow c$	m_c	0.407781159	0.407787380	15.256796	1.293413	1.273000	-15782.573	-0.00567(54)	0.4415(56)	0.4415(56)	16(18)
8	$\mu, u \rightarrow s$	m_b	0.441384763	0.441392989	18.635453	0.085012	0.083546	-17245.942	+0.02575(583)	0.518(10)	0.518(10)	16(120)
9	$\mu, \tau, d \rightarrow c$	2 GeV	0.387706554	0.387716195	24.866871	1.194975	1.170735	-20284.763	+0.01546(52)	0.63848(100)	0.63849(100)	17(12)
10	$\mu, \tau, s \rightarrow c$	m_b	0.341496792	0.341510567	40.338017	1.019592	1.047213	+27090.548	+0.05513(51)	0.5441(37)	0.5441(37)	33(21)

-
- [1] Y. Koide, Fermion-boson two-body model of quarks and leptons and Cabibbo mixing, *Lett. Nuovo Cim.* **34**, 201 (1982).
- [2] Y. Koide, New view of quark-lepton mass hierarchy, *Phys. Rev. D* **28**, 252 (1983).
- [3] S. Navas *et al.* (Particle Data Group), Review of particle physics, *Phys. Rev. D* **110**, 030001 (2024).
- [4] R. Foot, A note on Koide's lepton mass relation, *Mod. Phys. Lett. A* **9**, 169 (1994), arXiv:hep-ph/9402242.
- [5] Y. Sumino, Family gauge symmetry and Koide's mass formula, *Phys. Lett. B* **671**, 477 (2009), arXiv:0812.2090.
- [6] Y. Sumino, Family gauge symmetry as an origin of Koide's mass formula and charged lepton spectrum, *J. High Energy Phys.* **2009** (05), 075, arXiv:0812.2103.
- [7] N. Li and B.-Q. Ma, Estimate of neutrino masses from Koide's relation, *Phys. Lett. B* **609**, 309 (2005), arXiv:hep-ph/0505028.
- [8] N. Li and B.-Q. Ma, Energy scale independence of Koide's relation for quark and lepton masses, *Phys. Rev. D* **73**, 013009 (2006), arXiv:hep-ph/0601031.
- [9] Z.-z. Xing and H. Zhang, On the Koide-like relations for the running masses of charged leptons, neutrinos and quarks, *Phys. Lett. B* **635**, 107 (2006), arXiv:hep-ph/0602134.
- [10] W. Rodejohann and H. Zhang, Extended empirical fermion mass relation, *Phys. Lett. B* **698**, 152 (2011), arXiv:1101.5525.
- [11] A. Kartavtsev, A remark on the Koide relation for quarks, arXiv e-print (2011), unpublished preprint, arXiv:1111.0480.
- [12] G.-H. Gao and N. Li, Explorations of two empirical formulae for fermion masses, arXiv e-print (2015), unpublished preprint, arXiv:1512.06349.
- [13] A. Rivero and A. Gsponer, The strange formula of Dr. Koide, arXiv e-print (2005), unpublished preprint, arXiv:hep-ph/0505220.
- [14] C. A. Brannen, Spin path integrals and generations (2010), arXiv:1006.3114 [physics.gen-ph].
- [15] U.S. Department of Justice and Federal Trade Commission, *Horizontal Merger Guidelines*, Tech. Rep. (U.S. Department of Justice and Federal Trade Commission, 2010).
- [16] Z.-z. Xing, H. Zhang, and S. Zhou, Updated values of running quark and lepton masses, *Phys.*

- Rev. D **77**, 113016 (2008), arXiv:0712.1419 [hep-ph].
- [17] Y. Koide, Charged lepton mass sum rule from U(3) family higgs potential model, Mod. Phys. Lett. A **5**, 2319 (1990).
- [18] Y. Koide, Seesaw mass matrix model of quarks and leptons with flavor-triplet higgs scalars, Eur. Phys. J. C **48**, 223 (2006).
- [19] Y. Koide, Charged lepton mass relations in a supersymmetric yukawaon model, Phys. Rev. D **79**, 033009 (2009), arXiv:0811.3475 [hep-ph].